Colour figures

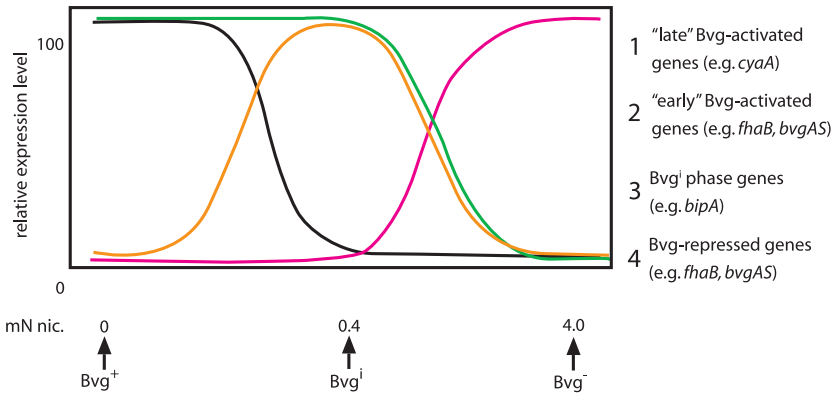

Fig. 2 Expression curves for the four classes of genes regulated by BvgAS. Genes expressed maximally in the Bvg$^+$ phase (such as *cyaA*) are referred to as "late" Bvg-activated genes and are represented by the black curve (curve 1). Genes that are expressed maximally under both Bvg$^+$ and Bvg^i phase conditions (such as *fhaB*) are referred to as "early" Bvg-activated genes and are represented by the green curve (curve 2). Genes expressed maximally only under Bvg^i phase conditions (such as *bipA*) are represented by the gold curve (curve 3). Finally, genes that are repressed by BvgAS and expressed maximally only under Bvg$^-$ phase conditions are represented by the red curve (curve 4). Abbreviation: nic, nicotinic acid. Adapted from Mattoo and Cherry, 2005.

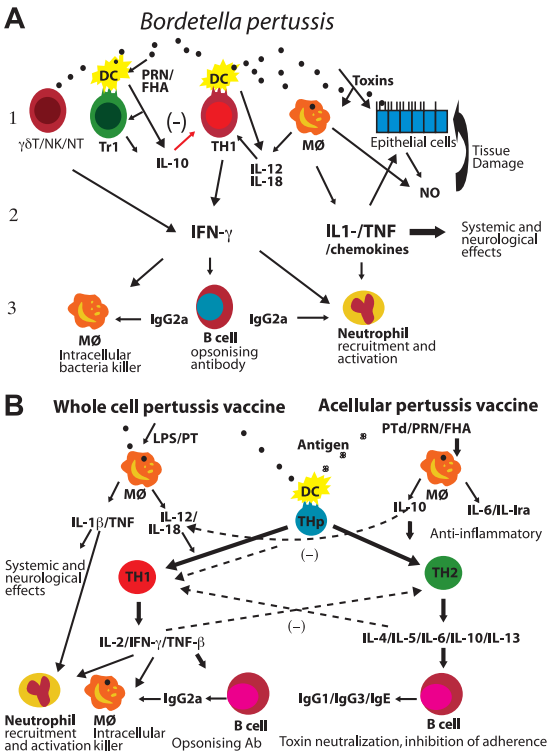

Fig. 4 (A) Immunity to *B. pertussis* in a naïve host: evidence from the murine respiratory challenge model. (1) Recognition of bacterial components by cells of the innate and acquired immune system, (2) Production of soluble mediators and (3) recruitment and activation of effector cells and molecules. When *B. pertussis* enters the respiratory tract, the bacteria bind to ciliated epithelial cells, but are also recognised and taken up by cells of the innate immune system, such as macrophages (Mϕ), dendritic cells (DCs), γδ T cells, natural killer (NK) or natural T cells (NT). DCs process and present bacterial antigens to T cells. The production of IL-12 and IL-18 by innate cells results in polarisation of the T-cell response to the Th1 subtype. However, early in infection the local Th1 response is suppressed due to the effects of IL-10 secreted by antigen-stimulated Tr1 cells or by FHA-stimulated macrophages and DCs. Nitric oxide (NO) and the pro-inflammatory cytokines, IL-1β and TNF-α induced by bacterial toxins, especially LPS, tracheal colonisation factor (TCT) and pertussis toxin (PT), as well as contributing to bacterial elimination, also mediate local lung pathology and are responsible for many of the systemic and neurological consequences of the infection. IFN-γ secreted early in infection by cells of the innate immune system, and later in infection by Th1 cells, stimulates recruitment and activation of macrophages and neutrophils and provides help for B cells to secrete opsonising and complement-fixing antibody (IgG2a in the mouse). Opsonised or non-opsonised bacteria are taken up by neutrophils and macrophages, which are killed by NO or reactive oxygen intermediates. (B) Distinct mechanisms of immunity induced with whole cell and acellular vaccines: a central role of Th1 and Th2 cells in regulation of the acquired immune response. wP include residual bacterial toxins, such as LPS, which activates IL-1β, TNF-α, IL-12 and IL-18 production by macrophages and other cells of the innate immune system. These pro-inflammatory cytokines regulate the selective induction of Th1 cells from the precursor T cell (Thp), but also contribute to the side effects of immunisation with wP. Cytokines secreted by Th1 cells, especially IFN-γ, provide help for opsonising antibody production and activate macrophages and neutrophils to take up and kill intracellular bacteria. In contrast, aP are devoid of bacterial toxins that stimulate IL-12 and IL-18, but include components such as FHA, which stimulate IL-10 production, and consequently have anti-inflammatory activity and preferentially induce Th2 cells. Th2 cells provide help for B cells to secrete IgE and murine IgG1, IgG3 antibodies, which neutralise toxins and prevent adherence of bacteria in the respiratory tract. Adapted from Mills *et al.*, 2001.

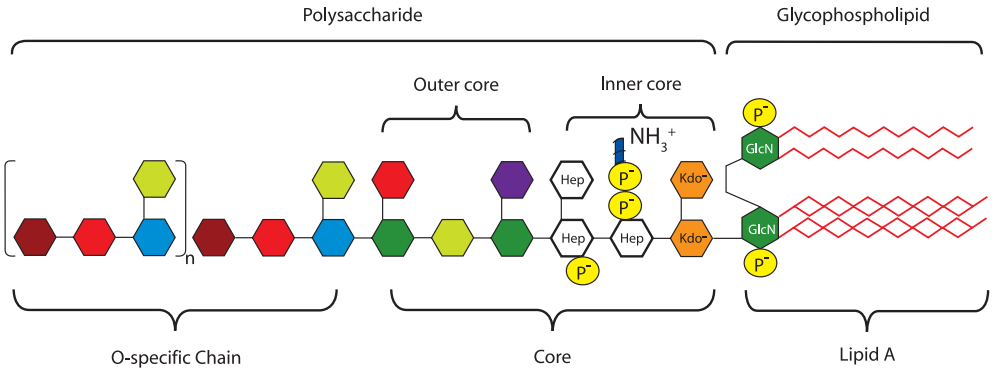

Fig. 5 Schematic representation of the chemical structure of enterobacterial LPS. Abbreviations: GlcN, glucosamine; Kdo, 2-keto-3-deoxyoctulosonic acid; Hep, L-glycero-D-manno-heptose; P, phosphate; EtN, ethanolamine; zigzag lines, fatty acids. Adapted from Caroff *et al.*, 2002.

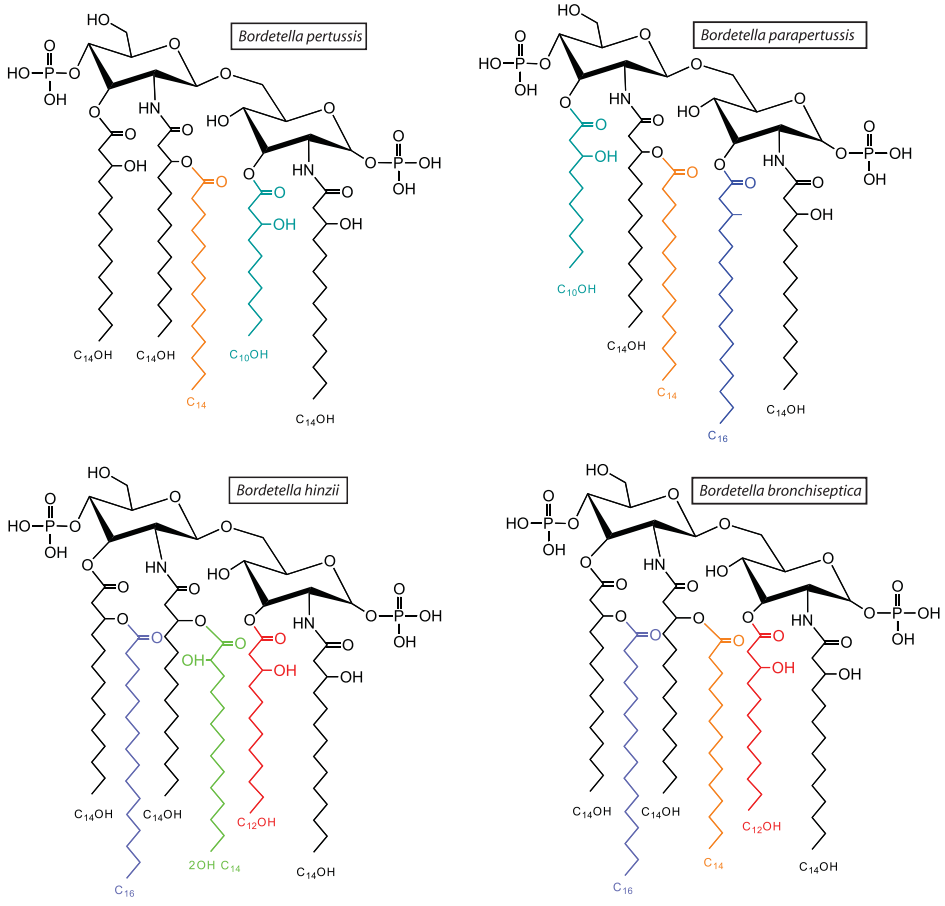

Fig. 7 Examples of lipid A structures from different *Bordetella* strains. Each colour indicates a specific fatty acid. Adapted from Caroff *et al.*, 2002.

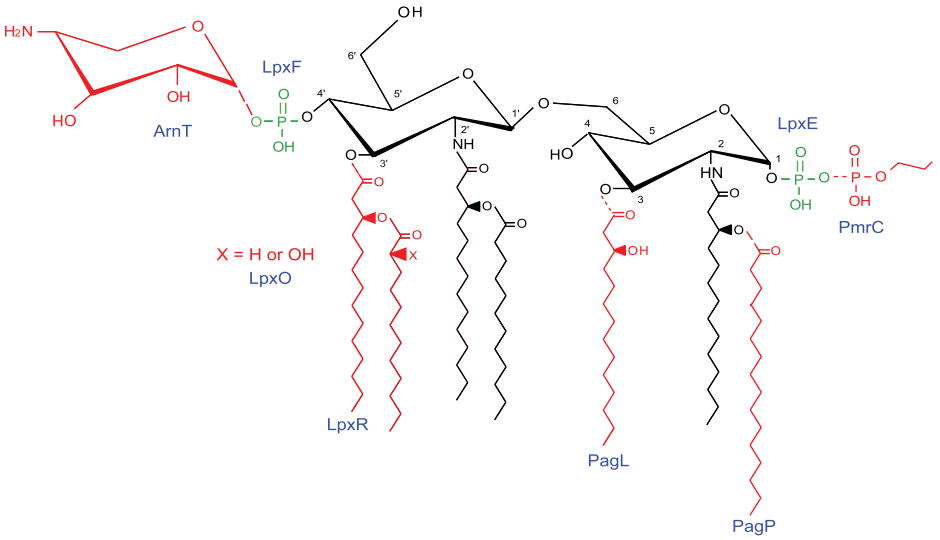

Fig. 9 Regulated modifications of lipid A. LpxE and LpxF function as 1- and 4'-phosphatases, respectively. Substitution of the phosphate moieties with L-Ara4N or pEtN is mediated by ArnT and PmrC, respectively, the formation of a 2-hydroxymyristate-modified lipid A by LpxO, the addition of a secondary palmitoyl chain at the 2-position by PagP, and the removal of the acyl chain moieties at the 3- and 3' position by PagL and LpxR, respectively.

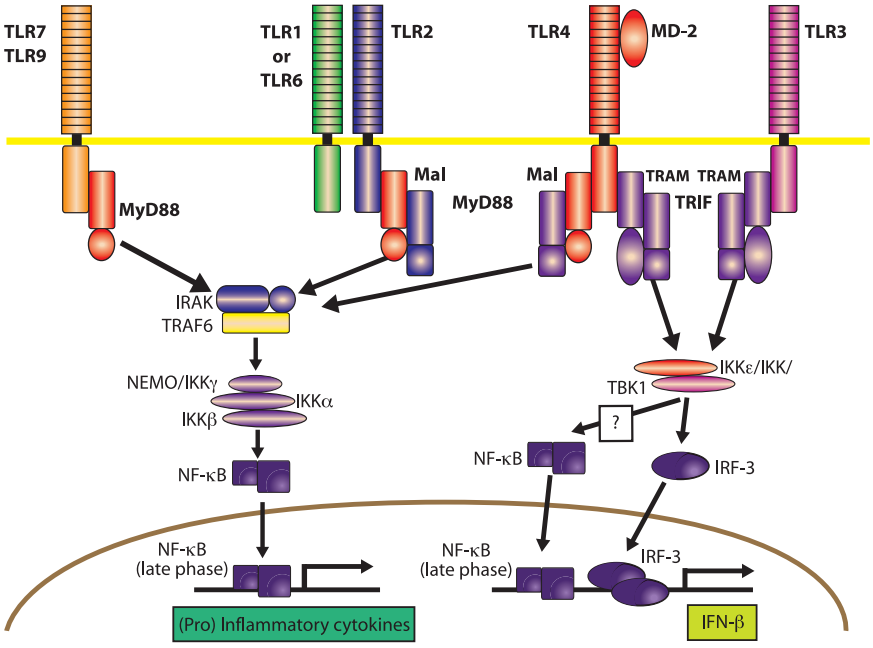

Fig. 10 TIR domain-containing adaptors and TLR signalling. MyD88 is an essential TIR domain-containing adaptor for the induction of inflammatory cytokines via the majority of TLRs. Mal is a second TIR domain-containing adaptor that specifically mediates the MyD88-dependent pathway via TLR2 and TLR4. In the TLR4- and TLR3-mediated signalling pathways, a MyD88-independent pathway exists that leads to activation of IRF-3 via TBK1 and IKKε/IKK*i*. The TIR domain-containing adaptor TRIF and the TRIF-related adapter molecule TRAM mediate this MyD88-independent pathway. Adapted from Takeda an Akira, 2004.

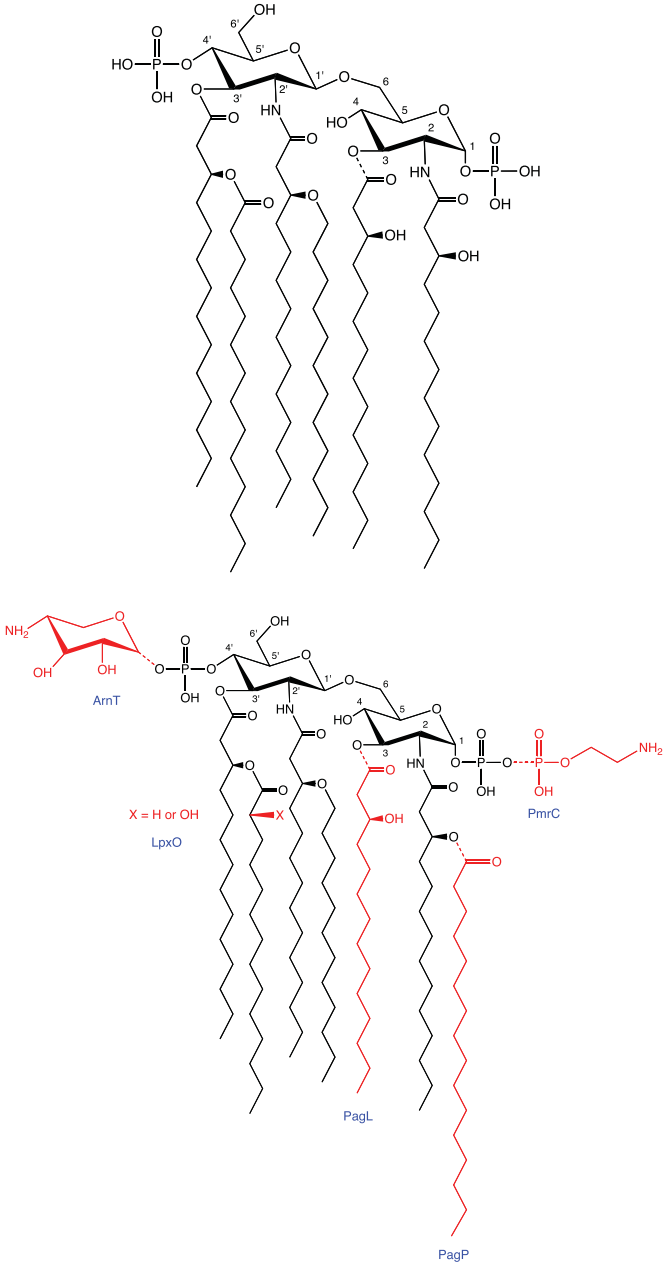

Fig. 1 Lipid A architecture. (A) *E. coli* lipid A consists of a bisphosphorylated glucosamine disaccharide substituted with four *R*-3-hydroxymyristoyl moieties, of which the 2'- and 3'-fatty-acyl chains are esterified with laurate and myristate, respectively. (B) regulated modifications of *Salmonella* lipid A. Substitution of the phosphate moieties with L-Ara4N or phosphoethanolamine is mediated by ArnT and PmrC, respectively, the formation of a 2-hydroxymyristate-modified lipid A by LpxO, the addition of a secondary palmitoyl chain at the 2 position by PagP, and the removal of the 3-hydroxymyristoyl moiety at the 3 position by PagL are shown.

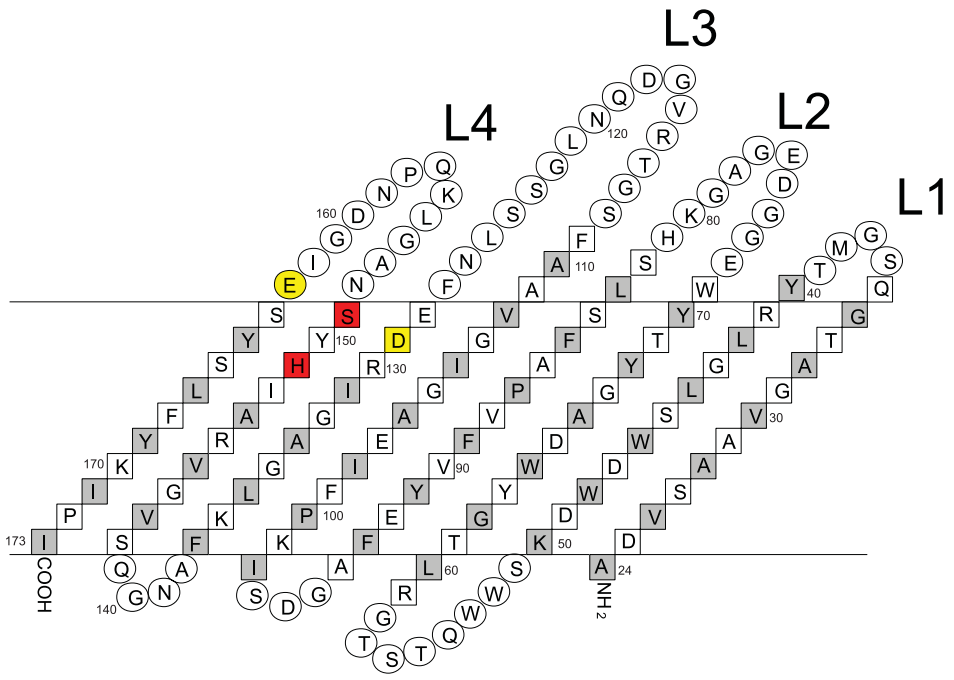

Fig. 8 Topology model for PagL from *P. aeruginosa*. A model for the topology of $PagL_{(Pa)}$ was constructed using the general rules of outer membrane protein architecture as described by Jacobs *et al*. (2003). The proposed model consists of an eight-stranded β-barrel with four loops (L1–4) extending into the external environment. Residues in the postulated β-strands are shown in diamonds, which are shaded for residues that are exposed to the lipid bilayers. His-149 and Ser-151 (marked in red; position in the $PagL_{(Pa)}$ precursor) are absolutely conserved (Fig. 2) and are suggested to be part of a classical catalytic triad of a serine hydrolase. Potential candidates for the acidic residue of the catalytic triad are indicated in yellow. Numbers refer to the positions of the residues in the precursor sequence.

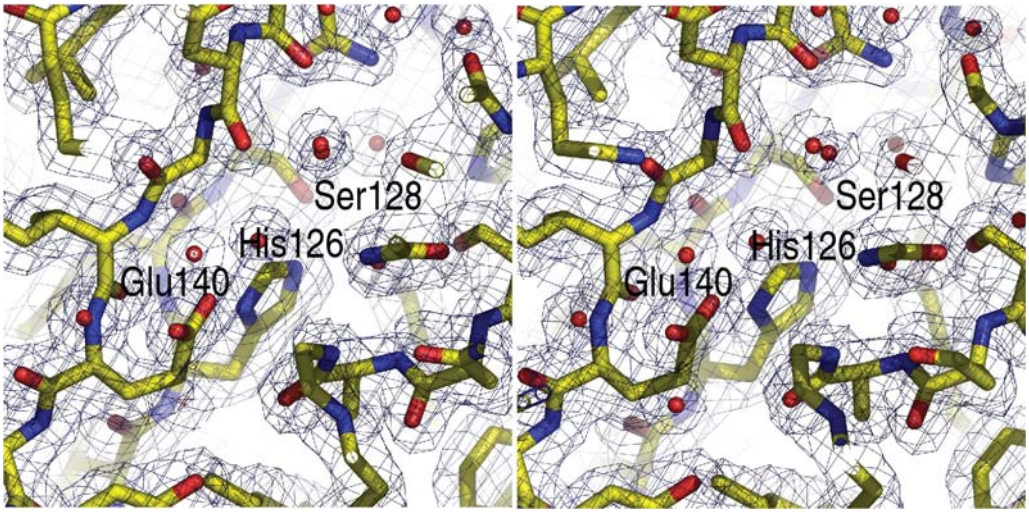

Fig. 1. Stereoview of the catalytic site with the final $2F_o$-F_c electron density map, at 2.0 Å resolution and contoured at 1σ, shown as chicken wire. Protein is shown as sticks. Carbon atoms are shown in yellow, oxygen in red and nitrogen in blue. Catalytic triad residues are labelled.

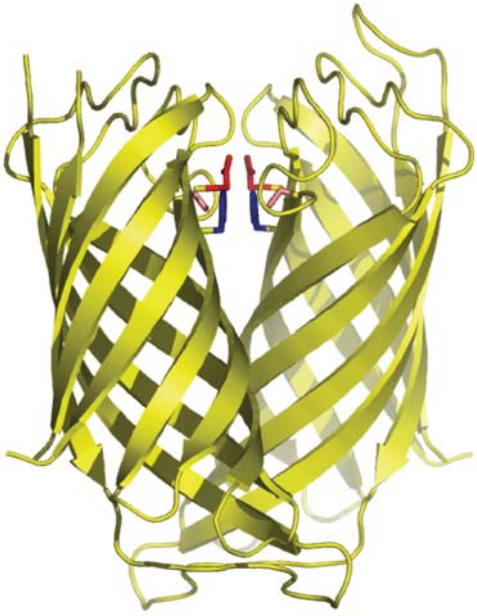

Fig. 4. PagL dimer in the crystal structure. The active-site residues Ser-128, His-126, and Glu-140 are coloured pink, blue, and red, respectively.

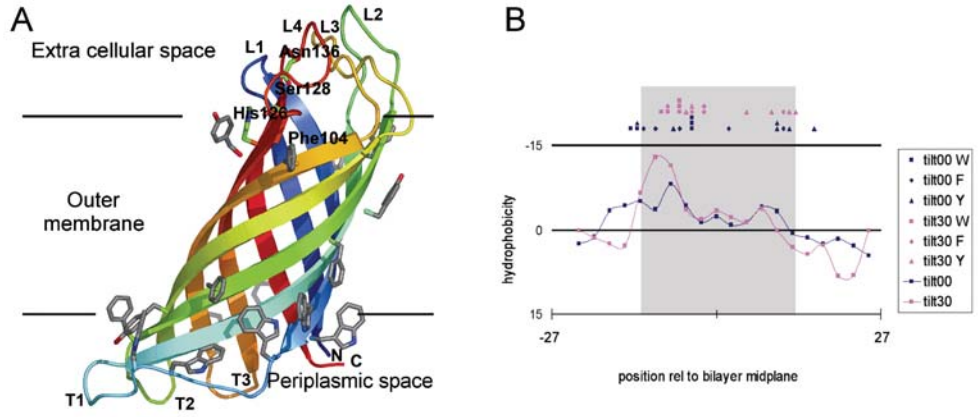

Fig. 5. PagL structure and membrane orientation. (A) Ribbon representation of PagL. The N and C termini are labelled and coloured blue and red, respectively, with gradient colours in between. The four extracellular loops are labelled L1–L4, and the three periplasmic turns are labelled T1–T3. Aromatic residues located at the presumed membrane boundaries are shown in gray, with nitrogen and oxygen atoms shown in blue and red, respectively. The only four completely conserved residues among PagL homologs are labelled. (B) Hydrophobicity profiles for the outward-facing PagL residues as a function of membrane position (periplasmic side left, extracellular side right) are shown as solid lines. Negative $\Sigma(\Delta G)$ values indicate regions that are more hydrophobic. The blue line and symbols present results for the positions with the β-barrel axis aligned along the membrane normal, whereas the magenta line and symbols are for the protein tilted by 30°. The symbols represent the Cγ positions of Trp (squares), Tyr (circles), and Phe (triangles) residues that form the inner and outer aromatic girdles. The image shown in (A) was prepared with PYMOL (www.pymol.org).

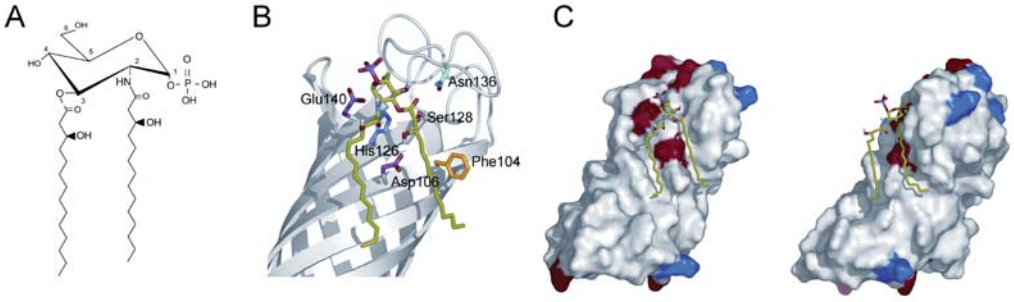

Fig. 8. Modelling of lipid X onto the active site of PagL. (A) Schematic representation of lipid X. (B) Lipid X modelled onto the active site of PagL. PagL is represented as a gray ribbon diagram. Lipid X is shown as green sticks with oxygen atoms in red and a phosphate atom in magenta. The hydrogen atoms from hydroxyl groups are shown in gray. Some amino acid residues important for PagL activity are shown as sticks and are labelled. (C) Two views (~90° rotated) of the electrostatic surface potential of PagL with lipid X. Positively and negatively charged residues are coloured blue and red, respectively. Lipid X is shown as green sticks. The images in *B* and *C* were prepared with PYMOL (www.pymol.org).

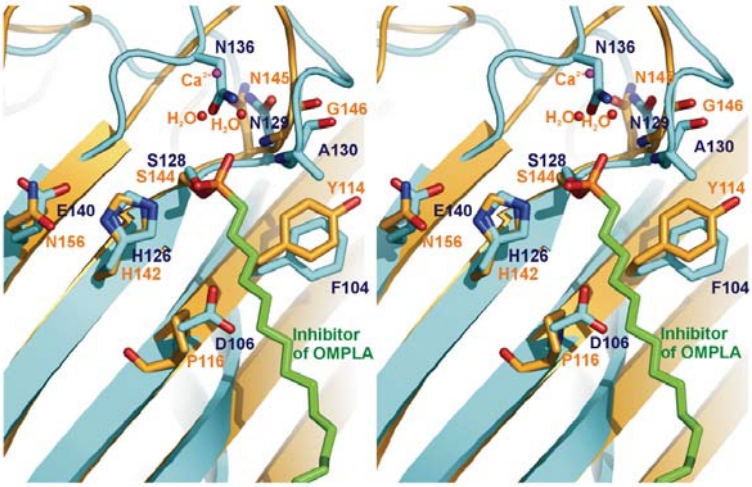

Fig. 9. Stereo diagram of the active site Ser-128 and His-126 of PagL superposed on the active site Ser-144 and His-142 of OMPLA. PagL is shown in cyan, whereas OMPLA is represented in orange. Residues and atoms that may have an important role for activity are shown as sticks and are labelled with cyan and orange text for PagL and OMPLA, respectively. The hexadecanesulfonyl moiety of an OMPLA inhibitor is covalently attached to Ser-144 of OMPLA and coloured green. The image was prepared by using PYMOL (www.pymol.org).

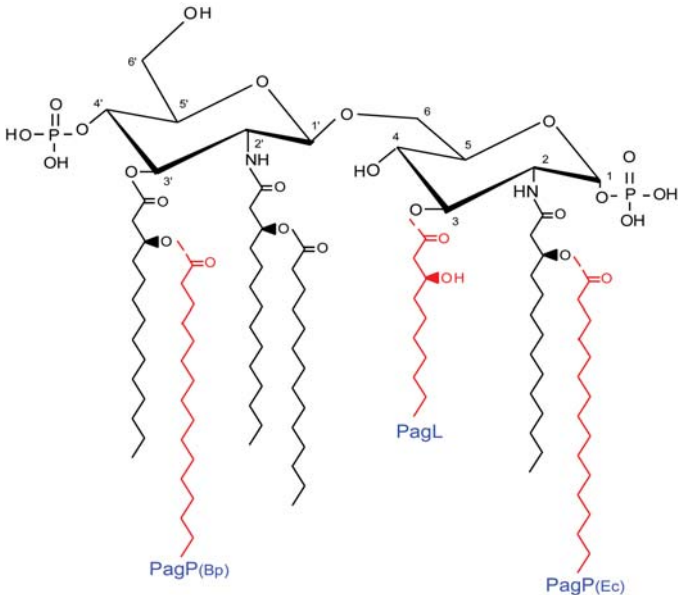

Fig. 1. *B. pertussis* lipid A architecture and modification by PagP and PagL. *B. pertussis* lipid A consists of a bisphosphorylated glucosamine disaccharide substituted with three *R*-3-hydroxytetradecanoic acid moieties and one *R*-3-hydroxydecanoic acid moiety, of which the 2' fatty acyl chain is esterified with myristate. *B. pertussis* PagP (PagP$_{(Bp)}$) and *E. coli* PagP (PagP$_{(Ec)}$) add a secondary palmitoyl chain at the 3' and 2 positions, respectively. Removal of the 3-hydroxydecanoic acid moiety at the 3 position is mediated by PagL.

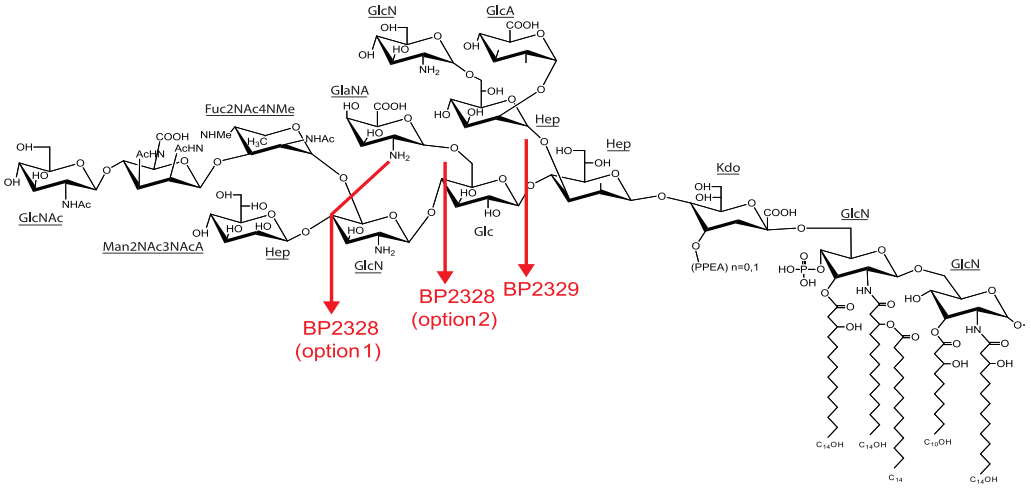

Fig. 7. Structure of *B. pertussis* LPS. Proposed truncated core OS structures of the BP2328- and BP2329-mutant strains are indicated by red arrows. Adapted from Caroff *et al*. (2000).